



MOUNTAIN WAVES IN THE MIDDLE ATMOSPHERE: MICROWAVE LIMB SOUNDER OBSERVATIONS AND ANALYSES

Jonathan H. Jiang¹, Dong L. Wu¹, Stephen D. Eckermann² and Jun Ma³

¹*Jet Propulsion Laboratory, California Institute of Technology, Pasadena, California 91109, USA*

²*Middle Atmospheric Dynamics Section, Naval Research Laboratory, Washington DC 20375, USA*

³*Computational Physics, Inc., Springfield, Virginia 22151, USA*

ABSTRACT

Observations and analyses of mesoscale gravity waves in the stratosphere from the Upper Atmosphere Research Satellite (UARS) Microwave Limb Sounder (MLS) are summarized, with focus on global distribution of topography related wave activities. We found most of the orographical wave activities occur during the winter seasons over high latitude mountain ridges. In the northern hemisphere, the strongest waves are those over Scandinavia, Central Eurasia, and southern Greenland, whereas in the southern hemisphere, wave activities are outstanding over the Andes, New Zealand, and Antarctic rim. MLS observations suggest that these orographic waves are located mostly on the down stream side of the mountain ridge with downward phase progression and have horizontal phase velocities opposite to the stratospheric jet-stream. Future studies using MLS data and numerical modeling will lead to better understanding of gravity wave effects on dynamics and chemistry in the middle atmosphere. © 2003 COSPAR. Published by Elsevier Ltd. All rights reserved.

BRIEF DESCRIPTION OF MLS GRAVITY WAVE VARIANCES

MLS 63GHz Saturated Radiances

UARS MLS measures O₂ radiances at 0-90 km tangent heights with 15 spectral channels. The radiances are mostly saturated when the instrument views tangent heights below ~18 km because of strong O₂ absorption. Radiances near the line center saturate at higher altitudes than those near the line wings. The saturated radiances are good measure of air temperature at the layer where the atmosphere becomes opaque. As the satellite and MLS line-of-sight (LOS) moves, fluctuations in the saturated radiances reflect atmospheric temperature variations induced by gravity waves (*Wu and Waters, 1997*).

MLS Gravity Wave Variances and Recent Improvements

The MLS gravity wave variance is computed from saturated limb radiances at the bottom of each scan for each channel (we call it *WW96 method* hereafter) described in *Wu and Waters, (1996a)*, and *Wu and Jiang, (2000)*. Several improvements since then have been made. First, we find that the tangent height cut-off needs to be below ~14 km in order for channel 1 radiances (saturating at the lowest altitude) to meet the saturation condition, which limits the number of independent measurements to be ≤ 4 for MLS normal limb scan operation. Thus, we choose to use the 4-point limb-scan variances in this study for more reliable gravity wave variances at lower altitudes, rather than 6-point variances used in *WW96 method*. For the limb-track case, we still use the 6-point variances but restrict measurements to those at tangent heights below ~18 km. The computed radiance variance has two components: instrument noise and atmospheric variance. The noise contribution is stable, well calibrated during the flight, and independent of time and location, thus can be easily removed (*Wu and Waters, 1997*). The atmospheric component, which reflects the air temperature fluctuations, is referred to as gravity wave variance.

Second, the signal-to-noise ratio (SNR) of the variances is improved by combining the radiances from a pair of channels that are symmetric about the line center. The symmetric channels have the similar temperature weighting function and noise figure and thus the variance from the combined radiances yields a noise level at about a half of that with the single channel radiances.

Third, we make a full use of the saturated radiances up to the highest tangent height. Instead of cutting off at 14 km tangent height for all the channels, we make the cutoff tangent height channel-dependent because radiances from different channels saturate at different heights. Higher cutoff heights may increase the number of samples for the variance.

Finally, we provided more accurate geographical locations for each radiance variance. Because the saturated radiances are measuring the atmospheric volume on the near side of the tangent point, the variance must be displaced from the tangent point for its geographical registration. This displacement was not considered in previous MLS gravity variance calculations and we found in studying mountain waves (Jiang *et al.* 2003) that distributions of wave activities are particularly sensitive to such error or displacement.

MLS Wave Filtering

Because the MLS weighting function has an “oval shape” and is tilted with respect to a local observer (Wu and Waters, 1997), the MLS wave filter function depends on wave propagation direction, horizontal and vertical wavelength. In UARS case, MLS gravity wave variances are available at 8 altitudes (28, 33, 38, 43, 48, 53, 61, and 80 km) and contributed mostly by waves of vertical wavelengths >10 km due to the instrument field-of-view filtering. Depending on the truncation length used, the derived GW variances can represent waves having wide range of horizontal wavelengths. For limb-scan observations (Wu and Waters, 1996a), the radiances are often truncated by 3-6 measurement points to meet the saturation criteria, which yield a horizontal scale of ~50-150 km. For limb-track (Wu and Waters, 1996b) observations, where the sequences of the saturated radiances are orbit-long, the truncation lengths can vary from a few tens km to as long as 1000+ km.

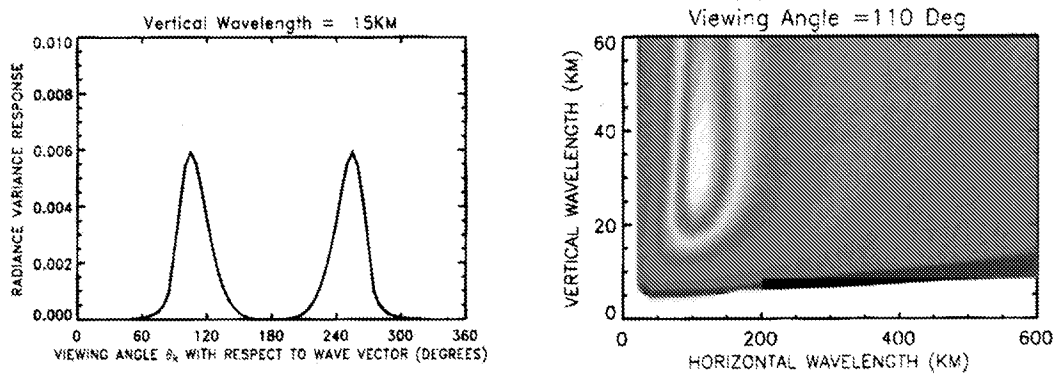


Figure 1: Simulated GW variance response as a function of viewing angle (left) and vertical/horizontal wavelength (right).

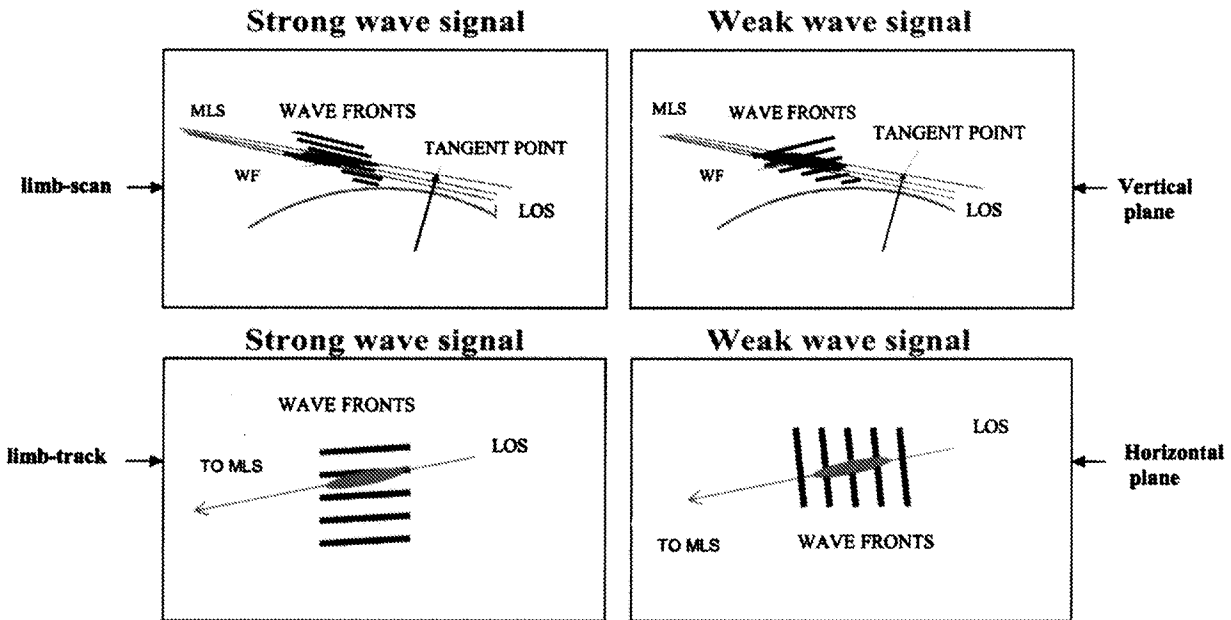


Figure 2: Examples of some MLS observation cases

Figure 1 shows examples of simulated MLS gravity wave variance response as a function of viewing angle (for a limb-track case) and as a function of vertical and horizontal wavelength (in the limb-scan case). The viewing angle is

defined as the angle between the LOS direction and the wave vector. Figure 2 illustrate examples of some MLS observation cases. From the simulations with a 2D MLS weighting function (*WF*, shown as oval-shape), we find that gravity wave variances are very sensitive to the direction in which waves are tilted as well as to the horizontal pattern of the wave fronts.

The filter function shown in Figure 1 also depends on the sampling schemes used. UARS MLS measurements were made with three distinct limb sampling patterns (Figure 3) that have different sensitivities to gravity waves. These data provide rich and unique information on how waves propagate into the upper-stratosphere and mesosphere, and are yet to be analyzed in further detail.

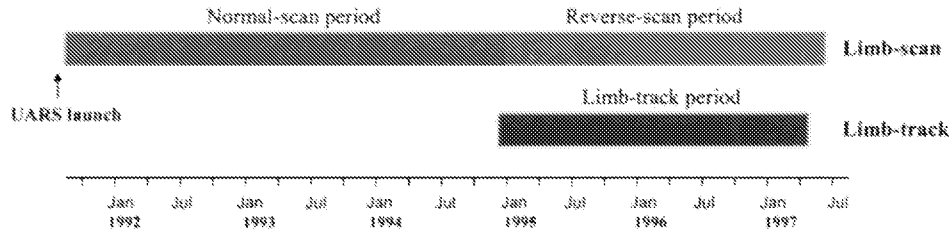


Figure 3: Periods of Different MLS Sampling Techniques

GRAVITY WAVES OBSERVED BY MLS

Global Distribution

Since mid-1990's, UARS MLS gravity wave variances have been used to study global distributions of meso-scale gravity waves in the stratosphere and mesosphere (*Wu and Waters, 1996a,b; Wu and Waters, 1997; Alexander, 1998; McLandress et al., 2000; Wu, 2001; Jiang and Wu, 2001; Wu and Jiang, 2002; Jiang et al., 2002*). Although the stratospheric background mean winds play an important role in filtering the gravity waves observed (*Alexander, 1998*), MLS gravity wave variances show good correlation with gravity wave sources near the surface, such as those connected to land topography (*Jiang et al., 2002*) and deep convection (*McLandress et al., 2000*).

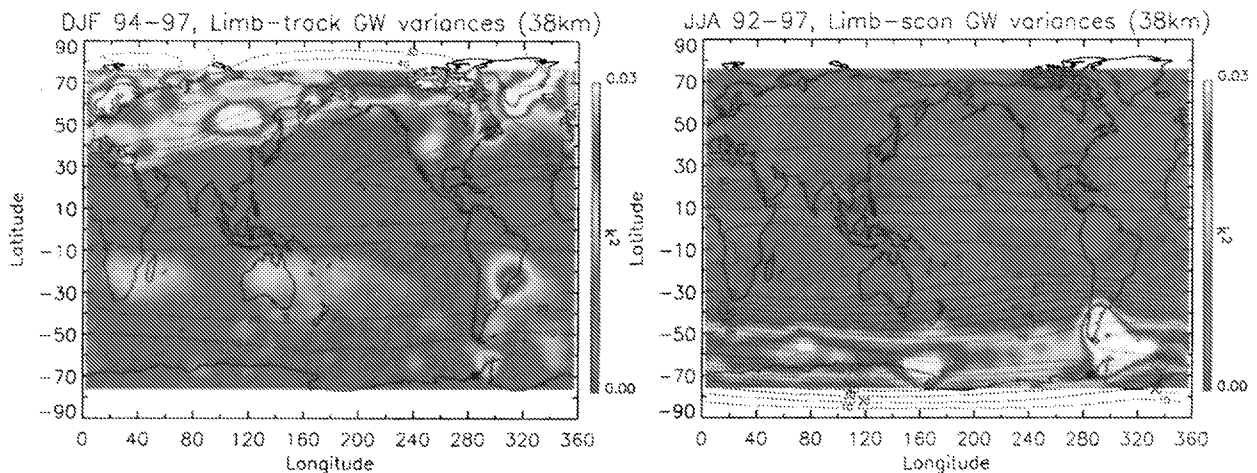


Figure 4: MLS observed global distribution of gravity waves. These waves have vertical and horizontal wavelenghts of $\lambda_z > 10$ km and $\lambda_x < 100$ km, respectively. The dotted contours lines are the 34-44 km mean UKMO winds (m/s).

Shown on the left in Figure 4 is an example of UARS MLS observed Northern Hemispheric winter gravity wave variances at altitude of 38 km. MLS limb-track data during December-February of 1994-1997 are averaged on 10°×5° longitude-latitude grids to make this map. The instrument noise has been removed. The map show topography related wave activities at high northern latitudes and convection-related wave activities in southern Africa, Australia and South America. Another example, shown in the right panel of Figure 4, is the Southern Hemispheric winter gravity wave variance map at 38 km, produced by averaging MLS limb-scan data during June-August of 1992-1997 on 10°×5° longitude-latitude grids. It shows strong wave activities over the southern Andes and around the Antarctica rim, as well

as some convection-related waves in the subtropics of the Northern Hemisphere, such as northern Africa, southern Asia, and Central America.

Mountain Waves in Winter Stratosphere

Both the stratospheric and tropospheric jet-streams prevail eastward in the wintertime Northern Hemisphere, which provides a favorable condition for high-latitude mountain waves to propagate into the stratosphere. Shown on the left panel of Figure 5 are MLS gravity wave variances in the Arctic winter stratosphere, at ~38 km altitude, measured from limb-track, north-looking descending orbits. Enhancements of gravity wave activities are clearly outstanding over the mountain ridges of Scandinavia, Urals, central Eurasia, Brooks Range of northern Alaska, Queen Elizabeth Islands of northern Canada, and southern Greenland. Note that unlike the left panel in Figure 4, the Northern Hemispheric map in Figure 5 are produced from measurements of the northern-looking, descending observing mode only, in which the mountain wave signals are most outstanding.

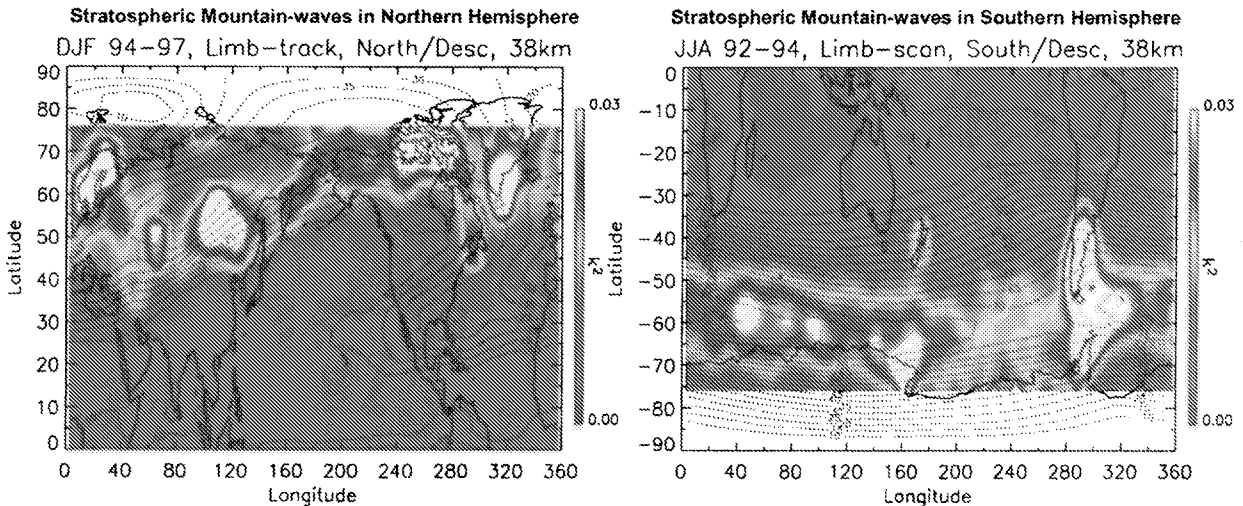


Figure 5: MLS observed mountain waves ($\lambda_z > 10$ km, $\lambda_x < 100$ km) in the wintertime stratosphere. Unlike Figure 4, results in Figure 5 are produced from different MLS observing modes, in order to highlight the mountain wave signals.

The right map in Figure 5 shows gravity wave variances at ~38 km during June-August of 1992-1997, observed from MLS limb-scan southern-looking descending orbits. The MLS gravity wave observations over the southern Andes provide a good example that satellite limb techniques can detect mountain waves generated by topography. Located near the edge of the stratospheric jet-stream, the southern Andes are often exposed to strong background winds during the Antarctic winter season, which allows gravity waves to propagate into the middle atmosphere. The wave activities are also significantly enhanced over the tip of the Antarctic Peninsula. The influence of the topography is extended in a long tail toward the east over Drake Passage, Scotia Sea and all the way along the Antarctica rim. Also, MLS shows good gravity wave sensitivity to pick up the weak signal over New Zealand.

MLS Inferred Wave Propagation Direction

From the simulations by *Wu and Waters* (1997), MLS gravity wave variances are sensitive to the direction of wave propagation, especially, to the direction where the wave vectors are tilted from zenith. In analysis of MLS gravity wave variances for various mountain waves, we found that the variances are usually high when observed on south-looking ascending or north-looking descending observation orbits; and low on south-looking descending or north-looking ascending orbits. Figure 6 shows examples of MLS observed mountain waves over the Rockies and southern Andes using data from different MLS observation modes. Mid-to-high latitudes of Northern Hemisphere, such as the Rockies region, are observable mainly from MLS northern-looking orbits. In the limb-scan example as shown in Figure 6, the gravity wave variances over the Rockies observed from descending orbits are substantially higher than the variances measured from ascending orbits. Since MLS line-of-sight (LOS) are looking toward slightly north of east direction at the Rockies latitudes (mostly eastward in low-latitudes) when on the north-looking descending orbits, the Figure 6 scenarios imply that vertically, a downward propagating wave front must be tilted toward west, or slightly south of west directions. At the turning latitudes (40°N) on south-looking orbits, where MLS line-of-sight are pointing almost directly southward, the gravity wave variances are about equal (or less different compared to north-looking cases) between ascending and descending situations, suggesting the horizontal component of the wave travels in the west-east direction, i.e. the wave fronts are lined up in south-north direction.

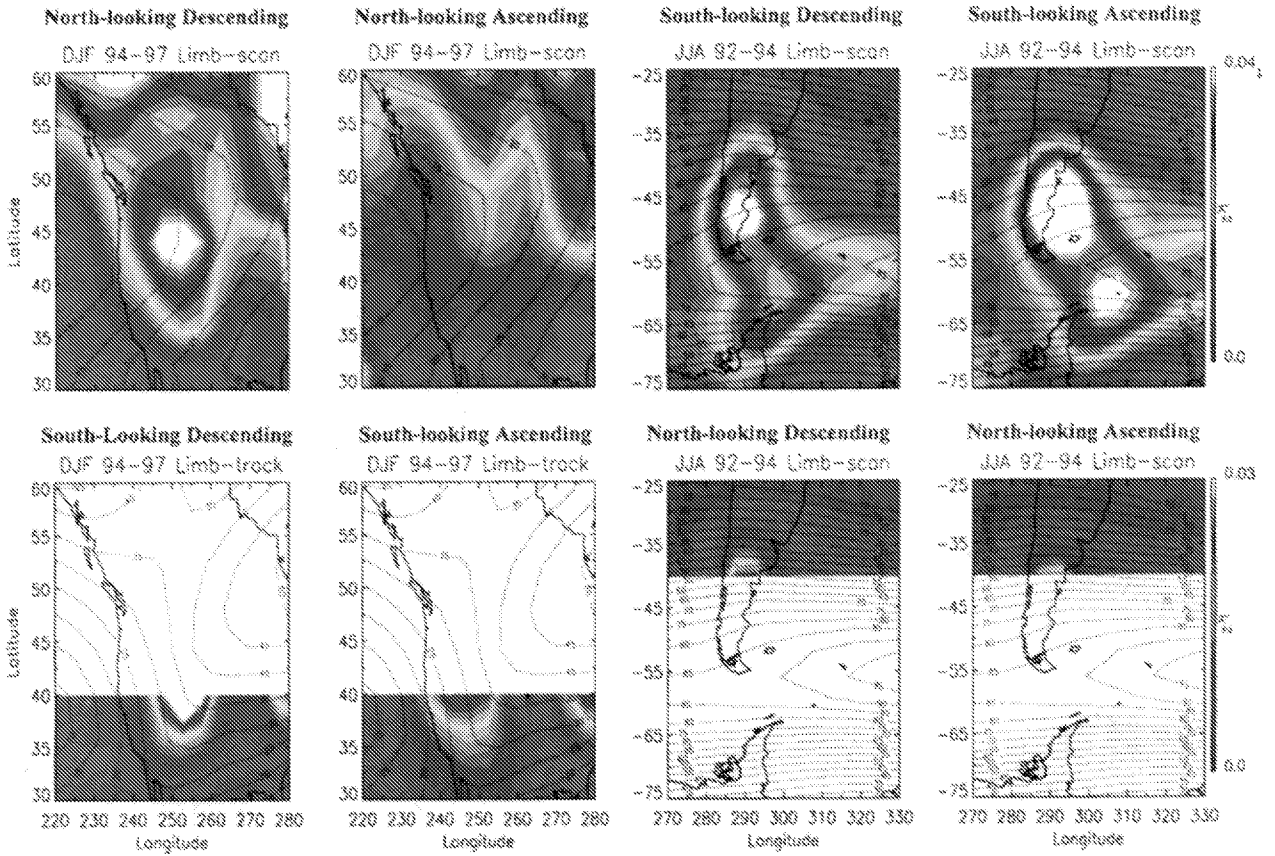
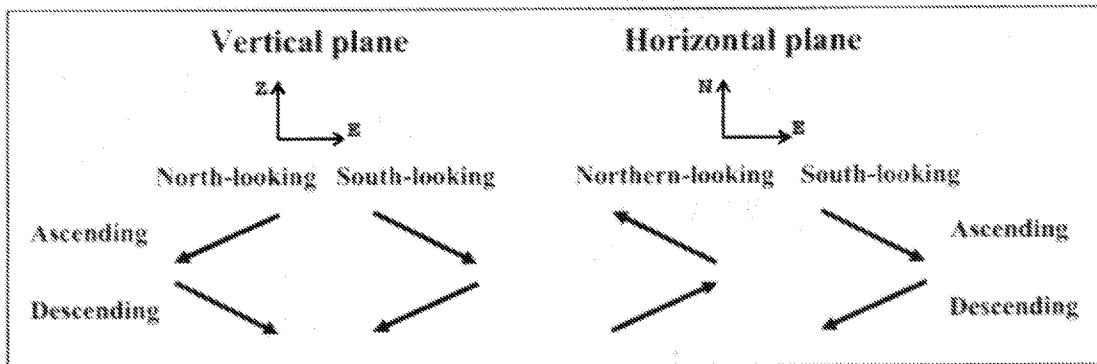


Figure 6: Regional maps of stratospheric mountain waves at 38 km over the Rockies (left two columns) and southern Andes (right two columns) produced using data from different MLS observing modes.

MLS Line-of-sight directions



Inferred wave propagation direction

MLS GW variances are higher under south-looking ascending or north-looking descending.
Wave propagation direction must be

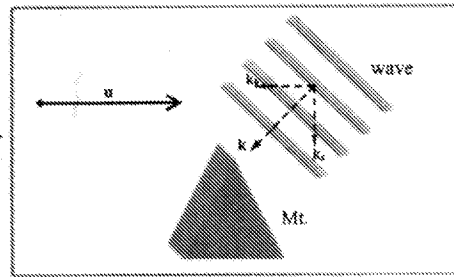


Figure 7: MLS inferred wave propagation direction

Similar analysis can also apply to gravity waves over the southern Andes (Figure 6, right panel). Together, these scenarios imply, as illustrated in Figure 7, that propagation direction of stratosphere mountain wave observed by MLS is tilted in such way that horizontal component of wave vector \mathbf{k}_h is opposite to wind vector \mathbf{u} . In other words, the mountain waves observed by MLS are dominated by downward phase propagating waves having horizontal phase velocities opposite to the stratospheric jet-streams.

COMPARISONS WITH NRL MOUNTAIN WAVE FORECAST MODEL

In recent studies, we found the seasonal and inter-annual variations of MLS radiance variances over many mountain ridges agree well with the simulations from the Naval Research Laboratory (NRL) Mountain Wave Forecast Model (MWFM) shown in Jiang *et al.* (2002, 2003). Jiang *et al.*, 2002 shows that the amplitude of the waves seems to correlate well with intensity of surface wind upstream of the Andes, which is related to the meridional temperature gradient in the region. This suggests that a climate anomaly event such as *El Niño* may play an important role in modulating the mountain wave generation and wave intensity reaching the stratosphere, an idea that MWFM also lends some support to.

Continuing investigations of these orographic waves with MWFM under realistic conditions could help us better interpolate the wave patterns observed by MLS and learn more about wave generation and propagation in the middle atmosphere.

CONCLUDING REMARKS

Through analyzing UARS MLS and upcoming Earth Observation Satellite (EOS) MLS gravity wave variances, we aim to achieve a better understanding of atmospheric gravity waves in these following areas: (1) Global GW sources and distributions; (2) Wave propagation properties and variations in the middle atmosphere; (3) Horizontal scale variations and relations to planetary waves; (4) Impacts on the formation of polar stratospheric clouds.

We hope to provide reliable global gravity wave observations to constrain the parameterizations used in general circulation models and enhance the model predictability. Also, many MLS gravity wave features remain unexplored and need better interpretation and understanding in the future studies.

ACKNOWLEDGMENTS

This study was supported by the Jet Propulsion Laboratory, California Institute of Technology, under contract with the National Aeronautics and Space Administration. The authors also acknowledge the support of the Naval Research Laboratory and the Computational Physics, Inc.

REFERENCES

- Alexander, M. J., Interpretation of observed climatological patterns in stratospheric gravity wave variance, *J. Geophys. Res.*, **103**, 8627-8640, 1998.
- Jiang, J. H., and D. L. Wu, UARS MLS observation of gravity waves associated with the Arctic winter stratospheric vortex, *Geophys. Res. Lett.*, **28**, 527-530, 2001.
- Jiang, J. H., D. L. Wu, S.D. Eckermann, Upper Atmosphere Research Satellite (UARS) MLS observation of mountain waves over the Andes, *J. Geophys. Res.* **107**, D22, 10.1029/2002JD002091, 2002.
- Jiang, J. H., S. D. Eckermann, D.L.Wu, and J. Ma, Stratospheric Mountain Waves in Northern Hemispheric Winter: UARS MLS observations compared with NRL MWFM simulations, manuscripts in preparation, 2003.
- McLandress, C., M. J. Alexander, D. L. Wu, Microwave Limb Sounder observations of gravity waves in the stratosphere: A climatology and interpretation, *J. Geophys. Res.*, **105**, 11947-11967, 2000.
- Wu, D. L., Horizontal wavenumber spectrum of MLS radiances, *J. Atmos. Solar-Terr. Phys.* **63**, 1465-1477, 2001.
- Wu, D. L., and J. H. Jiang, MLS observation of atmospheric gravity waves over Antarctica, *J. Geophys. Res.*, **107**, No. D24, 4773, 10.1029/2002JD002390, 2002.
- Wu, D. L. and J. H. Jiang, Mapping Atmospheric Gravity Wave Activity with Limb-Viewing Microwave Radiometer, *IEEE International Geoscience and Remote Sensing Symposium Proceedings*, 2000.
- Wu, D. L., and J. W. Waters, Satellite observations of atmospheric variances: A possible indication of gravity waves, *Geophys. Res. Lett.*, **23**, 3631-3634, 1996a.
- Wu, D. L., and J. W. Waters, Gravity-wave-scale temperature fluctuations seen by the UARS MLS, *Geophys. Res. Lett.*, **23**, 3289-3292, 1996b.
- Wu, D. L., and J. W. Waters, Observations of gravity waves with the UARS Microwave Limb Sounder, *Gravity Wave Processes, NATO ASI Series I: Global Environment Change*, **50**, 103-120, 1997.

Manuscript received October 11, 2002; revised January 22, 2003; accepted January 23, 2003.

E-mail address of Dr. Jonathan H. Jiang: jonathan@mls.jpl.nasa.gov